

Multimodal deep learning for short-term stock volatility prediction

Marcelo Sardelich^{a,*}, Suresh Manandhar^a

^a*Department of Computer Science Deramore Lane, University of York, Heslington, York, YO10 5GH, UK*

Abstract

Stock market volatility forecasting is a task relevant to assessing market risk. We investigate the interaction between news and prices for the one-day-ahead volatility prediction using state-of-the-art deep learning approaches. The proposed models are trained either end-to-end or using sentence encoders transferred from other tasks. We evaluate a broad range of stock market sectors, namely Consumer Staples, Energy, Utilities, Healthcare, and Financials. Our experimental results show that adding news improves the volatility forecasting as compared to the mainstream models that rely only on price data. In particular, our model outperforms the widely-recognized GARCH(1,1) model for all sectors in terms of coefficient of determination R^2 , MSE and MAE , achieving the best performance when training from both news and price data.

Keywords: deep learning, sequence learning, transfer learning, financial forecasting, volatility prediction, textual analysis, natural language preprocessing

PACS: 05.10.-a, 05.40.-a

2010 MSC: 62-07, 62H99

1. Introduction

Natural Language Processing (NLP) has increasingly attracted the attention of the financial community. This trend can be explained by at least three major factors. The first factor refers to the business perspective. It is the economics of gaining competitive advantage using alternative sources of data and going beyond historical stock prices, thus, trading by analyzing market news automatically. The second factor is the major advancements in the technologies to collect, store, and query massive amounts of user-generated data almost in real-time. The third factor refers to the progress made by the NLP community in understanding unstructured text.

*Corresponding author

Email addresses: marcelo.sardelich@york.ac.uk (Marcelo Sardelich), suresh@cs.york.ac.uk (Suresh Manandhar)

Over the last decades the number of studies using NLP for financial forecasting has experienced exponential growth. According to [1], until 2008, less than five research articles were published per year mentioning both “stock market” and “text mining” or “sentiment analysis” keywords. In 2012, this number increased to slightly more than ten articles per year. The last numbers available for 2016 indicates this has increased to sixty articles per year.

The ability to mechanically harvest the sentiment from texts using NLP has shed light on conflicting theories of financial economics. Historically, there has been two differing views on whether disagreement among market participants induces more trades. The “non-trade theorem” [2] states that assuming all market participants have common knowledge about a market event, the level of disagreement among the participants does not increase the number of trades but only leads to a revision of the market quotes. In contrast, the theoretically framework proposed in [3] advocates that disagreement among market participants increases trading volume. Using textual data from Yahoo and RagingBull.com message boards to measure the dispersion of opinions (positive or negative) among traders, it was shown in [4] that disagreement among users’ messages helps to predict subsequent trading volume and volatility. Similar relation between disagreement and increased trading volume was found in [5] using Twitter posts.

Additionally, textual analysis is adding to the theories of medium-term/long-term momentum/reversal in stock markets [6]. The unified Hong and Stein model¹ [7] on stock’s momentum/reversal proposes that investors underreact to news, causing slow price drifts, and overreact to price shocks not accompanied by news, hence inducing reversals. This theoretical predicated behaviour between price and news was systematically estimated and supported in [8, 9] using financial media headlines and in [10] using the Consumer Confidence Index[®] published by The Conference Board [11]. Similarly, [12] uses the *Harvard IV-4* sentiment lexicon to count the occurrence of words with positive and negative connotation of the *Wall Street Journal* showing that negative sentiment is a good predictor of price returns and trading volumes.

Accurate models for forecasting both price returns and volatility are equally important in the financial domain. Volatility measures how wildly the asset is expected to oscillate in a given time period and is related to the second moment of the price return distribution. In general terms, forecasting price returns is relevant to take speculative positions. The volatility, on the other hand, measures the risk of these positions. On a daily basis, financial institutions

¹The *gradual information diffusion* model of Hong and Stein considers two types of economic agents, namely “Newswatchers” and “Momentum traders”. The model consider three assumptions: 1) “Newswatchers” realize part of the public information and privately adjust their models, which are only based on macroeconomic and company specific forecasts. 2) “Momentum traders” only trade on past price performance. 3) Private, rather than public, information diffuses gradually, since each agent has a different time frame to adjust their models. These assumptions about market agents are enough to model the relationship between news and long-term trends or short-term reversals.

need to assess the short-term risk² of their portfolios. Measuring the risk is essential in many aspects. It is imperative for regulatory capital disclosures required by banking supervision bodies. Moreover, it is useful to dynamically adjust position sizing accordingly to market conditions, thus, maintaining the risk within reasonable levels.

Although, it is crucial to predict the short-term volatility from the financial markets application perspective, much of the current NLP research on volatility forecasting focus on the volatility prediction for very long-term horizons (see [13, 14, 15, 16, 17]). Predominately, these works are built on extensions of the bag-of-words representation that has the main drawback of not capturing word order. Financial forecasting, however, requires the ability to capture semantics that is dependent upon word order. For example, the headline “*Qualcomm sues Apple for contract breach*” and “*Apple sues Qualcomm for contract breach*” trigger different responses for each stock and for the market aggregated index, however, they share the same bag-of-words representation. Additionally, these works use features from a pretrained sentiment analysis model to train the financial forecasting model. A key limitation of this process is that it requires a labelled sentiment dataset. Additionally, the error propagation is not end-to-end.

In this work, we fill in the gaps of volatility prediction research in the following manner:

1. To move away from long-horizon volatility³ to short-term daily volatility prediction, we introduce a corpus of Reuters financial news. We compiled this corpus at individual stock level comprising the news titles (headlines) of 50 stocks in 5 diversified sectors with a total of 146,783 samples (2007–2017). We also collected daily stock prices from Yahoo Finance website for the 50 stocks.
2. We propose an end-to-end multimodal model that jointly learns from daily stock price and company news.
3. We investigate if the textual mode is complementary or redundant for the short-term volatility prediction problem. Our results indicate that textual mode is complementary and improves the forecasting accuracy.
4. We contribute to the Universal Sentence Representation works in [18, 19, 20] by comparing how transferable are the representations learnt in two different NLP tasks to the specific problem of volatility forecasting.
5. We propose a hierarchical *news relevance attention* mechanism that can effectively select the most relevant headline news from the large amount of news released in a given day.

²Usually, this risk is the conditional volatility for the next trading day

³The long-term forecast characteristic of the works described above is explained by the fact that the 10-K reports are only released annually.

2. Related work

Previous work in [13] incorporates sections of the “Form 10-K”⁴ to predict the volatility twelve months after the report is released. They train a Support Vector Regression model on top of sparse representation (bag-of-words) with standard term weighting (e.g. Term-Frequency). This work was extended in [14, 15, 16, 17] by employing the *Loughran-McDonald Sentiment Word Lists* [21], which contain three lists where words are grouped by their sentiments (positive, negative and neutral). In all these works, the textual representation is engineered using the following steps: 1) For each sentiment group, the list is expanded by retrieving 20 most similar words for each word using Word2Vec word embeddings [22]. 2) Finally, each 10-K document is represented using the expanded lists of words. The weight of each word in this sparse representation is defined using Information Retrieval (IR) methods such as *term-frequency* (tf) and *term-frequency with inverted document frequency* (tfidf). Particularly, [17] shows that results can be improved using enhanced IR methods and projecting each sparse feature into a dense space using Principal Component Analysis (PCA).

The works described above ([14, 15, 16, 17]) target long-horizon volatility predictions (one year or quarterly [17]). In particular, [17] and [16] uses market data (price) features along with the textual representation of the 10-K reports. These existing works that employ multi-modal learning [23] are based on a *late fusion*⁵ approach. For example, stacking ensembles to take into account the price and text predictions [17]. In contrast, our end-to-end trained model can learn the joint distribution of both price and text.

Predicting the price direction rather than the volatility was the focus in [24]. They extracted sentiment words from Twitter posts to build a time series of collective Profile of Mood States (POMS). Their results show that collective mood accurately predicts the direction of Dow Jones stock index (86.7% accuracy). In [25] handcrafted text representations including term count, noun-phrase tags and extracted named entities are employed for predicting stock market direction using Support Vector Machine (SVM). An extension of Latent Dirichlet Allocation (LDA) is proposed in [26] to learn a joint latent space of topics and sentiments.

Our deep learning models bear a close resemblance to works focused on directional price forecasting [27, 28]. In [27], headline news are processed using *Stanford OpenIE* to generate triples that are fed into a Neural Tensor Network to create the final headline representation. In [28], a character-level embedding is pre-trained in an unsupervised manner. The character embedding is used as

⁴Companies with listed stocks are enforced by the U.S. Securities and Exchange Commission (SEC) to file “Form 10-K” reports on an annual/quarterly basis. These forms provide an overview of the company’s business and financial health. A 10-K form example can be found [here](#)

⁵In the *late fusion* setup, text and price features are trained independently and a meta model is used in a later stage to discriminate how to weight the contribution of each mode.

input to a sequence model to learn the headline representation. Particularly, both works average all headline representations in a given day, rather than attempting to weight the most relevant ones. In this work, we propose a neural attention mechanism to capture the *News Relevance* and provide experimental evidence that it is a key component of the end-to-end learning process. Our attention extends the previous deep learning methods from [27, 28].

Despite the fact that end-to-end deep learning models have attained state-of-the-art performance, the large number of parameters make them prone to overfitting. Additionally, end-to-end models are trained from scratch requiring large datasets and computational resources. Transfer learning (TL) alleviates this problem by adapting representations learnt from a different and potentially weakly related source domain to the new target domain. For example, in computer vision tasks the convolutional features learnt from ImageNet [29] dataset (source domain) have been successfully transferred to multiple domain target tasks with much smaller datasets such as object classification and scene recognition [30].

In this work, we consider TL in our experiments for two main reasons. First, it address the question whether our proposed dataset is suitable for end-to-end training since the performance of the transferred representations can be compared with end-to-end learning. Second, it is still to be investigated which dataset transfers better to the forecasting problem. Recently, the NLP community has focused on universal representations of sentences [18, 20], which are dense representations that carry the meaning of a full sentence. [18] found that transferring the sentence representation trained on the Stanford Natural Language Inference (SNLI) [31] dataset achieves state-of-the-art sentence representations to multiple NLP tasks (e.g. sentiment analysis, question-type and opinion polarity). Following [18], in this work, we investigate the suitability of SNLI and Reuters RCV1 [32] datasets to transfer learning to the volatility forecasting task.

To the best of our knowledge, the hierarchical attention mechanism at headline level, proposed in our work, has not being applied to volatility prediction so far; neither has been investigated the ability to transfer sentence encoders from source datasets to the target forecasting problem (Transfer Learning).

3. Our dataset

Our corpus covers a broad range of news including news around earnings dates and complements the 10-K reports content. As an illustration, the headlines “*Walmart warns that strong U.S. dollar will cost \$15B in sales*” and “*Procter & Gamble Co raises FY organic sales growth forecast after sales beat*” describe the company financial conditions and performance from the management point of view – these are also typical content present in Section 7⁶ of the 10-K

⁶The section is called “Management’s Discussion and Analysis of financial conditions and results of operations” (MD&A), which is the management’s forward-looking section.

reports.

In this section, we describe the steps involved in compiling our dataset of financial news at stock level, which comprises a broad range of business sectors.

3.1. Sectors and stocks

The first step in compiling our corpus was to choose the constituents stocks. Our goal was to consider stocks in a broad range of sectors, aiming a diversified financial domain corpus. We found that Exchange Traded Funds (ETF) provide a mechanical way to aggregate the most relevant stocks in a given industry/-sector. An ETF is a fund that owns assets, e.g. stock shares or currencies, but, unlike mutual funds are traded in stock exchanges. These ETFs are extremely liquid and track different investment themes. We decided to use SPDR Setcor Funds constituents stocks in our work since the company is the largest provider of sector funds in the United States. We included in our analysis the top 5 (five) sector ETFs by financial trading volume (as in Jan/2018). Among the most traded sectors we also filtered out the sectors that were similar to each other. For example, the Consumer Staples and Consumer Discretionary sectors are both part of the parent Consumer category. For each of the top 5 sectors we selected the top 10 holdings, which are deemed the most relevant stocks. Table 1, details our dataset sectors and its respective stocks.

3.2. Stock specific data

We assume that an individual stock news as the one that explicitly mention the stock name or any of its *surface forms* in the headline. As an illustration, in order to collect all news for the stock code PG, *Procter & Gamble* company name, we search all the headlines with any of these words: **Procter&Gamble OR Procter and Gamble OR P&G**. In this example, the first word is just the company name and the remaining words are the company surface forms.

We automatically derived the surface forms for each stock by starting with a seed of surface forms extracted from the DBpedia Knowledge Base (KB). We then applied the following procedure:

- Relate each company name with the KB entity unique identifier.
- Retrieve all values of the `wikiPageRedirects` property. The property holds the names of different pages that points to the same entity/company name. This step sets the initial seed of surface forms.
- Manually, filter out some noisy property values. For instance, from the Procter & Gamble entity page we were able to automatically extract `dbr:Procter_and_gamble` and `dbr:P_&_G`, but had to manually exclude the noisy associations `dbr:Female_pads` and `dbr:California_Natural`.

The result of the steps above is a dictionary of surface forms wd_{sc} .

3.3. Stock headlines

Our corpus is built at stock code level by collecting headlines from the Reuters Archive. This archive groups the headlines by date, starting from 1 January 2007. Each headline is a html link (`<a href>` tag) to the full body of the news, where the *anchor text* is the headline content followed by the release time. For example, the page dated 16 Dec 2016 has the headline “*Procter & Gamble appoints Nelson Peltz to board 5:26PM UTC*”.

For each of the 50 stocks (5 sectors times 10 stocks per sector) selected using the criteria described in subsection 3.1, we retrieved all the headlines from the Reuters Archive ranging from 01/01/2007 to 30/12/2017. This process takes the following steps:

- For a given stock code (sc) retrieve all surface forms wd_{sc} .
- For each day, store only the headlines content matching any word in wd_{sc} . For each stored headline we also store the time and timezone.
- Convert the news date and time to Eastern Daylight Time (EDT)⁷.
- Categorize the news release time. We consider the following category set: `{before market, during market, after market, holidays, weekends}`. `during market` contains news between 9:30AM and 4:00PM. `before market` before 9:30AM and `after market` after 4:00PM.

The time categories prevents any misalignment between text and stock price data⁸. Moreover, it prevents data leakage and, consequently, unrealistic predictive model performance. In general, news released after 4:00PM EDT can drastically change market expectations and the returns calculated using close to close prices as in the GARCH(1,1) model (see Equation 1). Following [4], to deal with news misalignment, news issued after 4:00PM (`after market`) are grouped with the pre-market (`before market`) on the following trading day.

Table 2 shows the distribution of news per sector for each time category. We can see a high concentration of news released before the market opens (55% on average). In contrast, using a corpus compiled from message boards, a large occurrence of news during market hours was found [4]. This behaviour indicating day traders’ activity. Our corpus comprise financial news agency headlines, a content more focused on corporate events (e.g. lawsuits, merges & acquisitions, research & development) and on economic news (see Table 3 for a sample of our dataset). These headlines are mostly factual. On the other hand, user-generated content such as Twitter and message boards (as in [4, 5]) tends to be more subjective.

U.S. macroeconomic indicators such as *Retail Sales*, *Jobless Claims* and GDP are mostly released around 8:30AM (one hour before the market opens). These numbers are key drivers of market activity and, as such, have a high media

⁷The timezone of the New York Stock exchange

⁸Note that changing the timezone can change the original news date.

coverage. Specific sections of these economic reports impact several stocks and sectors. Another factor that contribute to the high activity of news outside regular trading hours are company earnings reports. These are rarely released during trading hours. Finally, before the market opens news agencies provide a summary of the international markets developments, e.g. the key facts during the Asian and Australian trading hours. All these factors contribute to the high concentration of pre-market news.

4. Background

We start this section by reviewing the GARCH(1,1) model, which is a strong benchmark used to evaluate our neural model. We then review the source datasets proposed in the literature that were trained independently and transferred to our volatility prediction model. Finally, we review the general architectures of sequence modelling and attention mechanisms.

4.1. GARCH model

Financial institutions use the concept of “Value at risk” to measure the expected volatility of their portfolios. The widespread econometric model for volatility forecasting is the Generalized Autoregressive Conditional Heteroskedasticity (GARCH) [33, 34]. Previous research shows that the GARCH(1,1)⁹ model is hard to beat. For example, [35] compared GARCH(1,1) with 330 different econometric volatility models showing that they are not significantly better than GARCH(1,1). Let p_t be the price of an stock at the end of a trading period with closing returns r_t given by

$$r_t = \frac{p_t}{p_{t-1}} - 1 \quad (1)$$

The GARCH process explicitly models the time-varying volatility of asset returns. In the GARCH(1,1) specification the returns series r_t follow the process:

$$r_t = \mu + \epsilon_t \quad (2)$$

$$\epsilon_t = \sigma_t z_t \quad (3)$$

$$\sigma_t^2 = a_0 + a_1 \epsilon_{t-1}^2 + b_1 \sigma_{t-1}^2 \quad (4)$$

where μ is a constant (return drift) and z_t is a sequence of i.i.d. random variables with mean zero and unit variance. It is worth noting that although the conditional mean return described in Equation 2 has a constant value, the conditional volatility σ_t is time-dependent and modeled by Equation 31.

⁹The GARCH(p,q) model is specified in terms of the number of lagged terms p and q . The GARCH(1,1) specification considers only one lagged volatility ($p = 1$) and shock ($q = 1$) terms.

4.1.1. Forecasting

The one-step ahead expected volatility forecast can be computed directly from Equation 4 and is given by

$$E_T[\sigma_{T+1}^2] = a_0 + a_1 E_T[\epsilon^2] + b_1 E_T[\sigma_T^2] \quad (5)$$

In general, the t' -steps ahead expected volatility $E_T[\sigma_{T+t'}^2]$ can be easily expressed in terms of the previous step expected volatility. It is easy to prove by induction that the forecast for any horizon can be represented in terms of the one-step ahead forecast and is given by

$$E_T[\sigma_{T+t'}^2] - \sigma_u^2 = (a_1 + b_1)^{(t'-1)} (E_T[\sigma_{T+1}^2] - \sigma_u^2) \quad (6)$$

where σ_u is the *unconditional volatility*:

$$\sigma_u = \sqrt{a_0 / (1 - a_1 - b_1)} \quad (7)$$

From the equation above we can see that for long horizons, i.e. $t' \rightarrow \infty$, the volatility forecast in Equation 6 converges to the unconditional volatility in Equation 7.

All the works reviewed in section 1 ([13, 14, 15, 16, 17]) consider GARCH(1,1) benchmark. However, given the long horizon of their predictions (e.g. quarterly or annual), the models are evaluated using the unconditional volatility σ_u in Equation 7. In this work, we focus on the short-term volatility prediction and use the GARCH(1,1) one-day ahead conditional volatility prediction in Equation 5 to evaluate our models.

4.1.2. Evaluation

Let σ_{t+1} denote the ex-post “true” daily volatility at a given time t . The performance on a set with N daily samples can be evaluated using the standard Mean Squared Error (*MSE*) and Mean Absolute Error (*MAE*)

$$MSE = \frac{1}{N} \sum_{t=1}^N (E_t[\sigma_{t+1}] - \sigma_{t+1})^2 \quad (8)$$

$$MAE = \frac{1}{N} \sum_{t=1}^N |E_t[\sigma_{t+1}] - \sigma_{t+1}| \quad (9)$$

Additionally, following [36], the models are also evaluated using the coefficient of determination R^2 of the regression

$$\sigma_{t+1} = a + b E_t[\sigma_{t+1}] + e_t \quad (10)$$

where

$$R^2 = 1 - \frac{\sum_{t=1}^N e_t^2}{\sum_{t=1}^N \left(E_t[\sigma_{t+1}] - \frac{1}{N} \sum_{t=1}^N E_t[\sigma_{t+1}] \right)^2} \quad (11)$$

One of the challenges in evaluating GARCH models is the fact that the ex-post volatility σ_{t+1} is not directly observed. Apparently, the squared daily returns r_{t+1}^2 in Equation 1 could stand as a good proxy for the ex-post volatility. However, the squared returns yield very noisy measurements. This is a direct consequence of the term z^t that connects the squared return to the latent volatility factor in Equation 3. The use of intraday prices to estimate the ex-post daily volatility was first proposed in [36]. They argue that volatility estimators using intraday prices is the proper way to evaluate the GARCH(1,1) model, as opposed to squared daily returns. For example, considering the Deutsche Mark the GARCH(1,1) model R^2 improves from 0.047 (squared returns) to 0.33 (intraday returns)¹⁰ [36].

4.1.3. Range measures to daily volatility proxy

It is clear from the previous section that any volatility model evaluation using the noisy squared returns as the ex-post volatility proxy will lead to very poor performance. Therefore, high-frequency intraday data is fundamental to short-term volatility performance evaluation. However, intraday data is difficult to acquire and costly. Fortunately, there are statistically efficient daily volatility estimators that only depend on the open, high, low and close prices. These price “ranges” are widely available. In this section, we discuss these estimators.

Let O_t , H_t , L_t , C_t be the open, high, low and close prices of an asset in a given day t . Assuming that the daily price follows a geometric Brownian motion with zero drift and constant daily volatility σ , Parkinson (1980) derived the first daily volatility estimator

$$\widehat{\sigma_{PK,t}^2} = \frac{\ln\left(\frac{H_t}{L_t}\right)^2}{4\ln(2)} \quad (12)$$

which represents the daily volatility in terms of its price range. Hence, it contains information about the price path. Given this property, it is expected that σ_{PK} is less noisy than the volatility calculated using squared returns. The Parkinson’s volatility estimator was extended by Garman-Klass (1980) which incorporates additional information about the opening (O_t) and closing (C_t) prices and is defined as

$$\widehat{\sigma_{GK,t}^2} = \frac{1}{2} \ln\left(\frac{H_t}{L_t}\right)^2 - (2\ln(2) - 1) \ln\left(\frac{C_t}{O_t}\right)^2 \quad (13)$$

The relative noisy of different estimators $\hat{\sigma}$ can be measured in terms of its relative efficiency to the daily volatility σ and is defined as

$$e\left(\widehat{\sigma^2}, \sigma^2\right) \equiv \frac{Var[\sigma^2]}{Var[\widehat{\sigma^2}]} \quad (14)$$

¹⁰The intraday estimator is calculated using squared returns of price data sampled every 5 minutess.

where $\text{Var}[\cdot]$ is the variance operator. It follows directly from Equation 3 that the squared return has efficiency 1 and therefore, very noisy. [37] reports Parkinson $(\widehat{\sigma_{PK,t}^2})$ volatility estimator has 4.9 relative efficiency and Garman-Klass $(\widehat{\sigma_{GK,t}^2})$ 7.4. Additionally, all the described estimators are unbiased.

Many alternative estimators to daily volatility have been proposed in the literature. However, experiments in [37] rate the Garman-Klass volatility estimator as the best volatility estimator based only on open, high, low and close prices. In this work, we train our models to predict the state-of-the-art Garman-Klass estimator. Moreover, we evaluate our models and GARCH(1,1) using the metrics described in subsection 4.1.2, but with the appropriate volatility proxies, i.e. Parkinson and Garman-Klass estimators.

4.2. Transfer Learning from other source domains

Vector representations of words, also known as Word embeddings [22, 38], that represent a word as a dense vector has become the standard building blocks of almost all NLP tasks. These embeddings are trained on large unlabeled corpus and are able to capture context and similarity among words.

Some attempts have been made to learn vector representations of a full sentence, rather than only a single word, using unsupervised approaches similar in nature to word embeddings. Recently, [18] showed state-of-the-art performance when a sentence encoder is trained end-to-end on a supervised source task and transferred to other target tasks. Inspired by this work, we investigate the performance of sentence encoders trained on the Text categorization and Natural Language Inference (NLI) tasks and use these encoders in our main short-term volatility prediction task.

A generic sentence encoder S_e receives the sentence words as input and returns a vector representing the sentence. This can be expressed as a mapping

$$S_e: \mathbb{R}^{T^S \times d_w} \rightarrow \mathbb{R}^{d_S} \quad (15)$$

from a variable size sequence of words to a sentence vector S of fixed-size d_S , where T^S is the sentence number of words and d_w is the pre-trained word embedding dimension.

In the following sections, we describe the datasets and architectures to train the sentence encoders of the auxiliary transfer learning tasks.

4.2.1. Reuters RCV1

The Reuters Corpus Volume I (RCV1) is corpus containing 806,791 news articles in the English language collected from 20/08/1996 to 19/08/1997 [32]. The topic of each news was human-annotated using a hierarchical structure. At the top of the hierarchy, lies the coarse-grained categories: CCAT (Corporate), ECAT (Economics), GCAT (Government), and MCAT (Markets). A news article can be assigned to more than one category meaning that the text categorization task is multilabel. Each news is stored in a separate XML file. Listing 1 shows the typical structure of an article.

```

<?xml version="1.0" encoding="iso-8859-1" ?>
<newsitem itemid="6159" id="root" date="1996-08-21" xml:lang="en">
<headline>Colombia raises internal coffee price.</headline>
<dateline>BOGOTA 1996-08-21</dateline>
<copyright>(c) Reuters Limited 1996</copyright>
<metadata>
<codes class="bip:topics:1.0">
  <code code="C13">
    <editdetail attribution="Reuters_BIP_Coding_Group" action="
      confirmed" date="1996-08-21" />
  </code>
  <code code="C31">
    <editdetail attribution="Reuters_BIP_Coding_Group" action="
      confirmed" date="1996-08-21" />
  </code>
  <code code="CCAT">
    <editdetail attribution="Reuters_BIP_Coding_Group" action="
      confirmed" date="1996-08-21" />
  </code>
  <code code="M14">
    <editdetail attribution="Reuters_BIP_Coding_Group" action="
      confirmed" date="1996-08-21" />
  </code>
  <code code="M141">
    <editdetail attribution="Reuters_BIP_Coding_Group" action="
      confirmed" date="1996-08-21" />
  </code>
  <code code="MCAT">
    <editdetail attribution="Reuters_BIP_Coding_Group" action="
      confirmed" date="1996-08-21" />
  </code>
</codes>
</metadata>
</newsitem>

```

Listing 1: **RCV1 dataset article example.** For brevity’s sake, we only show the markup consumed in our models. This headline has root categories CCAT (Corporate/Industrial) and MCAT (Markets) with direct children categories C13 (REGULATION/POLICY), C31 (MARKETS/MARKETING) and M14 (COMMODITY MARKETS). The last category M141 (SOFT COMMODITIES) is a children of M14 and describes the commodity market type.

The RCV1 dataset is not released with a standard train, validation, test split. In this work, we separated 15% of samples as a test set for evaluation purposes. The remaining samples were further split leaving 70% and 15% for training and validation, respectively.

Regarding the categories distribution, we found that, from the original 126 categories, 23 categories were never assigned to any news; therefore, were disregarded. From the 103 classes left we found a high imbalance among the labels with a large number of underrepresented categories having less than 12 samples. The very low number of samples for these minority classes brings a great challenge to discriminate the very fine-grained categories. Aiming to alleviate this problem, we grouped into a same class all categories below the second hierarchical level. For example, given the root node CCAT (Corporate) we grouped C151 (ACCOUNTS/EARNINGS), C1511 (ANNUAL RESULTS)

and C152 (COMMENT/FORECASTS) into the direct child node C15 (PERFORMANCE). Using this procedure the original 103 categories were reduced to 55. One of the benefits of this procedure was that the less represented classes end up having around thousand samples compared with only 12 samples in the original dataset.

Figure 1, shows the architecture for the end-to-end text categorization task. On the bottom of the architecture S_e receives word embeddings and outputs a sentence vector S . The S vector passes through a fully connected (FC) layer with sigmoid activation function that outputs a vector $\hat{y} \in \mathbb{R}^{55}$ with each element $\hat{y}_j \in [0, 1]$.

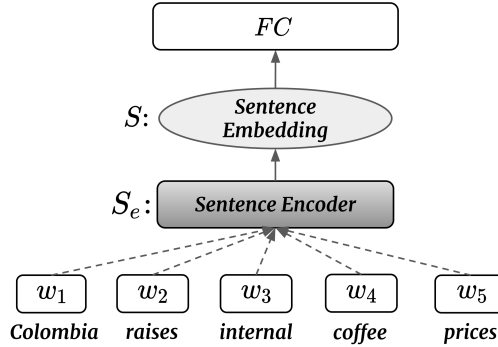


Figure 1: **RCV1 text categorization architecture.** The sentence encoder S_e maps word embeddings w_i to a sentence vector S and the last FC layer has a sigmoid activation function.

The architecture described above is trained under the assumption that each category is independent but not mutually exclusive since a sample can have more than one category assigned (multilabel classification). The loss per sample is the average *log loss* across all labels:

$$\mathcal{L}(\hat{y}, y) = - \sum_{i=1}^{55} (y_i \log(\hat{y}_i) + (1 - y_i) \log(1 - \hat{y}_i)) \quad (16)$$

where the index i runs over the elements of the predicted and true vectors.

Given the high categories imbalance, during the training we monitor the F_1 metric of the validation set and choose the model with the highest value.

4.2.2. SNLI dataset

Stanford Natural Language Inference (SNLI) dataset [31] consist of 570,000 pairs of sentences. Each pair has a premise and a hypothesis, manually labeled with one of the three labels: *entailment*, *contradiction*, or *neutral*. The SNLI has many desired properties. The labels are equally balanced, as opposed to the

RCV1 dataset. Additionally, language inference is a complex task that requires a deeper understanding of the sentence meaning making this dataset suitable for learning supervised sentence encoders that generalize well to other tasks [18]. Table 4, shows examples of SNLI dataset sentence pairs and its respective labels.

In order to learn sentence encoders that can be transferred to other tasks unambiguously, we consider a neural network architecture for the sentence encoder with shared parameters between the premise and hypothesis pairs as in [18].

Figure 2, describes the neural network architecture. After each premise and hypothesis is encoded into S_p and S_h , respectively, we have a fusion layer. This layer has no trainable weights and just concatenate each sentence embedding. Following [18], we add two more matching methods: the absolute difference $|S_p - S_h|$ and the element-wise $S_p \odot S_h$. Finally, in order to learn the pair representation, S_{ph} is feed into an FC layer with rectified linear unit (ReLU) activation function, which is expressed as $f(x) = \log(1 + e^x)$. The last softmax layer outputs the probability of each class.

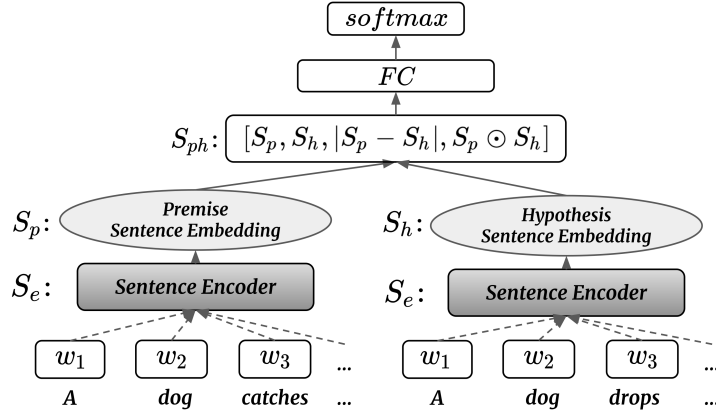


Figure 2: **Natural Language Inference task architecture.** Note that the sentence encoder S_e is shared between the premise and hypothesis pair. The FC layer learns the representation of the sentence pair and the final Softmax layer asserts the output of the 3 possible labels, i.e. $[entailment, contradiction, neutral]$, sums to one.

Finally, the NLI classifier weights are optimized in order to minimize the categorical log loss per sample

$$\mathcal{L}(\hat{y}, y) = - \sum_{j=1}^3 y_j \log(\hat{y}_j) \quad (17)$$

During the training, we monitor the validation set accuracy and choose the model with the highest metric value.

4.3. Sequence Models

We start this section by reviewing the Recurrent Neural Network (RNN) architecture and its application to encode a sequence of words.

RNN's are capable of handling variable-length sequences, this being a direct consequence of its recurrent cell, which shares the same parameters across all sequence elements. In this work, we adopt the Long Short-Term Memory (LSTM) cell [39] with forget gates f_t [40]. The LSTM cell is endowed with a memory state that can learn representations that depend on the order of the words in a sentence. This makes LSTM more fit to find relations that could not be captured using standard bag-of-words representations.

Let x_1, x_2, \dots, x_T be a series of observations of length T , where $x_t \in \mathbb{R}^{d_w}$. In general terms, the LSTM cell receives a previous hidden state h_{t-1} that is combined with the current observation x_t and a memory state C_t to output a new hidden state h_t . This internal memory state C_t is updated depending on its previous state and three modulating gates: input, forget, and output. Formally, for each step t the updating process goes as follows (see Figure 3 for a high level schematic view): First, we calculate the input i_t , forget f_t , and output o_t gates:

$$i_t = \sigma_s(W_i x_t + U_i h_{t-1} + b_i) \quad (18)$$

$$f_t = \sigma_s(W_f x_t + U_f h_{t-1} + b_f) \quad (19)$$

$$o_t = \sigma_s(W_o x_t + U_o h_{t-1} + b_o) \quad (20)$$

where σ_s is the sigmoid activation. Second, a candidate memory state \tilde{C}_t is generated:

$$\tilde{C}_t = \tanh(W_c x_t + U_c h_{t-1} + b_c) \quad (21)$$

Now we are in a position to set the final memory state C_t . Its value is modulated based on the input and forget gates of Equation 20 and is given by:

$$C_t = i_t \odot \tilde{C}_t + f_t \odot C_{t-1} \quad (22)$$

Finally, based on the memory state and output gate of Equation 20, we have the output hidden state

$$h_t = o_t \odot \tanh(C_t) \quad (23)$$

Regarding the trainable weights, let n be the LSTM cell number of units. It follows that W 's and U 's matrices of the affine transformations have $n \times d_w$ and $n \times n$ dimensions, respectively. Its bias terms b 's are vectors of size n . Consequently, the total number of parameters is $4(nd_w + n^2 + n)$ and does not depend on the sequence number of time steps T .

We see that the LSTM networks are able to capture temporal dependencies in sequences of arbitrary length. One straightforward application is to model the Sentence encoder discussed in subsection 4.2, which outputs a sentence vector representation using its words as input.

Given a sequence of words $\{w_t\}_{t=1}^T$ we aim to learn the words hidden state $\{h_t\}_{t=1}^T$ in a way that each word captures the influence of its past and future words. The Bidirectional LSTM (BiLSTM) proposed in [41] is an LSTM that

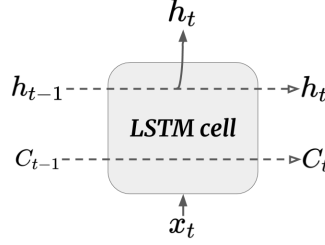


Figure 3: **Schematic view of a LSTM cell.** The observed state x_t is combined with previous memory and hidden states to output a hidden state h_t . The memory state C_t is an internal state; therefore, not part of the output representation. An LSTM network is trained by looping its shared cell across all sequence length.

“reads” a sentence, or any sequence in general, from the beginning to the end (forward) and the other way around (backward). The new state h_t is the concatenation

$$h_t = [\vec{h}_t, \overleftarrow{h}_t] \quad (24)$$

where

$$\vec{h}_t = \text{LSTM}(w_1, \dots, w_T) \quad (25)$$

$$\overleftarrow{h}_t = \text{LSTM}(w_T, \dots, w_1) \quad (26)$$

$$(27)$$

Because sentences have different lengths, we need to convert the T concatenated hidden states of the BiLSTM into a fixed-length sentence representation. One straightforward operation is to apply any form of pooling. Attention mechanism is an alternative approach where the sentence is represented as an weighted average of hidden states where the weights are learnt end-to-end.

In the next sections we describe the sentence encoders using pooling and attention layers.

4.3.1. BiLSTM max-pooling

The max-pooling layer aims to extract the most salient word features all over the sentence. Formally, it outputs a sentence vector representation $S_{MP} \in \mathbb{R}^{2n}$ such that

$$S_{MP} = \max_{t=1}^T h_t \quad (28)$$

where h_t is defined in Equation 24 and the max operator is applied over the time steps dimension. Figure 4 illustrates the BiLSTM max-pooling (MP) sentence encoder.

The efficacy of the max-pooling layer was assessed in many NLP studies. [42] employed a max-pooling layer on top of word representations and argues that it performs better than mean pooling. Experimental results in [18] show that

among three types of pooling (max, mean and last¹¹) the max-pooling provides the most universal sentence representations in terms of transferring performance to other tasks. Grounded on these studies, in this work, we choose the BiLSTM max-pooling as our pooling layer of choice.

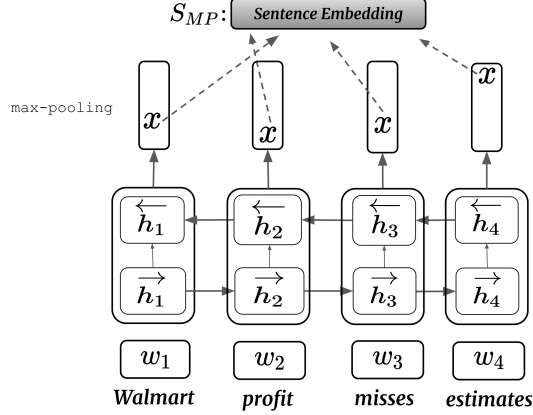


Figure 4: **BiLSTM max-pooling**. The network performs a polling operation on top of each word hidden state.

4.3.2. BiLSTM attention

Attention mechanisms were introduced in the deep learning literature to overcome some simplifications imposed by pooling operators. When we humans read a sentence, we are able to spot its most relevant parts in a given context and disregard information that is redundant or misleading. The attention model aims to mimic this behaviour.

Attention layers were proposed for different NLP tasks. For example, NLI, with cross-attention between premise and hypothesis, Question & Answering and Machine Translation (MT). Specifically in the Machine Translation task, each word in the target sentence learns to attend the relevant words of the source sentence in order to generate the sentence translation.

A sentence encoder with attention (or self-attentive) [43, 44, 45] assigns different weights to the own words of the sentence; therefore, converting the hidden states into a single sentence vector representation.

Considering the word hidden vectors set $\{h_1, \dots, h_T\}$ where $h_t \in \mathbb{R}^n$, the

¹¹The “last” polling is a simple operator that takes only the last element of the T hidden states to represent a sentence.

attention mechanism is defined by the equations:

$$\tilde{h}_t = \sigma(W h_t + b) \quad (29)$$

$$\alpha_t = \frac{\exp(v^\top \cdot \tilde{h}_t)}{\sum_t \exp(v \cdot \tilde{h}_t)} \quad (30)$$

$$S_{A_w} = \sum_t \alpha_t h_t \quad (31)$$

where $W \in \mathbb{R}^{d_a \times n}$, $b \in \mathbb{R}^{d_a \times 1}$, and $v \in \mathbb{R}^{d_a \times 1}$ are trainable parameters.

We can see that the sentence representation S_{A_w} is a weighted average of the hidden states. Figure 5 provides a schematic view of the BiLSTM attention, where we can account the attention described in Equation 31 as a two layer model with a dense layer (d_a units) followed by another dense that predicts α_t (single unit).

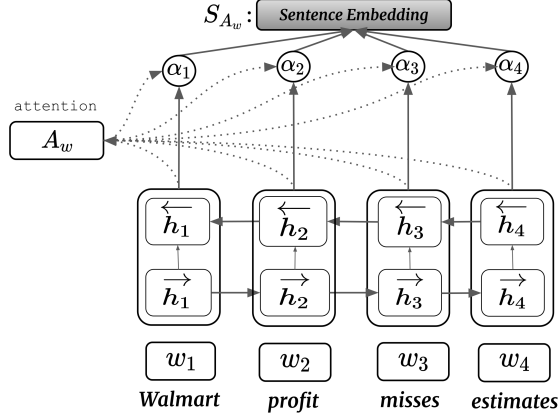


Figure 5: **BiLSTM attention**. The specific example encodes a headline from our corpus.

5. Methodology

In this section, we first introduce our problem in a deep multimodal learning framework. We then present our neural architecture, which is able to address the problems of news relevance and novelty. Finally, we review the methods applied to learn commonalities between stocks (global features).

5.1. Problem statement

Our problem is to predict the daily stock volatility. As discussed in subsubsection 4.1.3, the Gaman-Klass estimator $\widehat{\sigma_{GK,t}}$ in Equation 13 is a very efficient short-term volatility proxy, thus, it is adopted as our target variable.

Our goal is to learn a mapping between the next day volatility σ_{t+1} and historical multimodal data available up to day t . To this aim, we use a *sliding window* approach with window size T . That is, for each stock sc a sample on day t is expressed as a sequence of historical prices P_t^{sc} and corpus headlines N_t^{sc} . The price sequence is a vector of Daily Prices (DP) and expressed as

$$P_t^{sc} = [DP_{t-T}^{sc}, DP_{t-T+1}^{sc}, \dots, DP_t^{sc}] \quad (32)$$

where $DP_{t'}^{sc}$ is a vector of price features. In order to avoid task-specific feature engineering, the daily price features are expressed as the simple returns:

$$DP_t^{sc} = \left[\frac{O_t^{sc}}{C_{t-1}^{sc}} - 1, \frac{H_t^{sc}}{C_{t-1}^{sc}} - 1, \frac{L_t^{sc}}{C_{t-1}^{sc}} - 1, \frac{C_t^{sc}}{C_{t-1}^{sc}} - 1 \right] \quad (33)$$

The sequence of historical corpus headlines N_t^{sc} is expressed as

$$N_t^{sc} = [n_{t-T}^{sc}, n_{t-T+1}^{sc}, \dots, n_t^{sc}] \quad (34)$$

where $n_{t'}^{sc}$ is a set containing all headlines that influence the market on a given day t' .

Aiming to align prices and news modes, we consider the *explicit alignment* method discussed in subsection 3.3. That is, $n_{t'}^{sc}$ contains all stock headlines before the market opens (**before market_t**), during the trading hours (**during market_t**), and previous day after-markets (**after market_{t-1}**).

As a text preprocessing step, we tokenize the headlines and convert each word to an integer that refers to its respective pre-trained word embedding. This process is described as follows: First, for all stocks of our corpus we tokenize each headline and extract the corpus vocabulary set V . We then build the embedding matrix $E_w \in \mathbb{R}^{|V| \times d_w}$, where each row is a word embedding vector d_w dimensions. Words that do not have a corresponding embedding, i.e. out of vocabulary words, are skipped.

Finally, the input sample of the text mode is a tensor of integers with $T \times l_n \times l_s$ dimensions, where l_n is the maximum number of news occurring in a given day and l_s is the maximum length of a corpus sentence. Regarding the price mode, we have a $T \times 4$ tensor of floating numbers.

5.2. Global features and stock embedding

Given the price and news histories for each stock sc we could directly learn *one model per stock*. However, this approach suffers from two main drawbacks. First, the market activity of one specific stock is expected to impact other stocks, which is a widely accepted pattern named “spillover effect”. Second, since our price data is sampled on a daily basis, we would train the stock model relying on a small number of samples. One possible solution to model the commonality among stocks would be *feature enrichment*. For example, when modeling a given stock X we would enrich its news and price features by concatenating features

from stock Y and Z . Although the feature enrichment is able to model the effect of other stocks, it still would consider only one sample per day.

In this work, we propose a method that learns an *global model*.

The global model is implemented using the following methods:

- **Multi-Stock batch samples:** Since our models are trained using Stochastic Gradient Descent, we propose at each mini-batch iteration to sample from a batch set containing any stock of our stocks universe. As a consequence, the mapping between volatility and multimodal data is now able to learn common explanatory factors among stocks. Moreover, adopting this approach increases the total number of training samples, which is now the sum of the number of samples per stock.
- **Stock Embedding:** Utilizing the Multi-Stock batch samples above, we tackle the problem of modeling commonality among stocks. However, it is reasonable to assume that stocks have part of its dynamic driven by idiosyncratic factors. Nevertheless, we could aggregate stocks per sector or rely on any measure of similarity among stocks. In order to incorporate information specific to each stock, we propose to equip our model with a “stock embedding” mode that is learnt jointly with price and news modes. That is to say, we leave the task of distinguishing the specific dynamic of each stock to be learnt by the neural network. Specifically, this stock embedding is modeled using a discrete encoding as input, i.e. \mathcal{I}_t^{sc} is a vector with size equal to the number of stocks of the stocks universe and has element 1 for the i -th coordinate and 0 elsewhere, thus, indicating the stock of each sample.

Formally, we can express the one model per stock approach as the mapping

$$\sigma_{t+1}^{sc} = f^{sc}(DN_{t-T}^{sc}, DN_{t-T+1}^{sc}, \dots, DN_t^{sc}; DP_{t-T}^{sc}, DP_{t-T+1}^{sc}, \dots, DP_t^{sc}) \quad (35)$$

where $DN_{t'}^{sc}$ is a fixed-vector representing all news released on a given day for the stock sc ¹² and $DP_{t'}^{sc}$ is defined in Equation 33.

The global model attempts to learn a single mapping f that at each mini-batch iteration randomly aggregates samples across all the universe of stocks, rather than one mapping f^{sc} per stock. The global model is expressed as

$$\sigma_{t+1}^{sc} = f(DN_{t-T}^{sc}, DN_{t-T+1}^{sc}, \dots, DN_t^{sc}; DP_{t-T}^{sc}, DP_{t-T+1}^{sc}, \dots, DP_t^{sc}; \mathcal{I}_t^{sc}) \quad (36)$$

In the next section, we describe our hierarchical neural model and how the news, price and stock embedding are fused into a joint representation.

¹²It will become clear in the next section how this news representation is modelled.

5.3. Our multimodal hierarchical network

In broad terms, our hierarchical neural architecture is described as follows. First, each headline released on a given day t is encoded into a fixed-size vector S_t using a sentence encoder¹³. We then apply our daily New Relevance Attention (NRA) mechanism that attends each news based on its content and converts a variable size of news released on a given day into a single vector denoted by Daily News (DN). We note that this representation take account of the overall effect of all news released on a given day. This process is illustrated in Figure 6. We now are in a position to consider the temporal effect of the past T days of market news and price features. Figure 7 illustrates the neural network architecture from the temporal sequence to the final volatility prediction. For each stock code sc the temporal encoding for news is denoted by Market News MN_t^{sc} and for the price by Market Price MP_t^{sc} and are a function of the past T Daily News representations $\{DN_{t-T}^{sc}, \dots, DN_t^{sc}\}$ (**Text mode**) and Daily Prices features $\{DP_{t-T}^{sc}, \dots, DP_t^{sc}\}$ (**Price mode**), where each Daily Price DP_t^{sc} feature is given by Equation 33 and the DN_t^{sc} representation is calculated using **Daily New Relevance Attention**. After the temporal effects of T past days of market activity were already encoded into the Market News MN_t^{sc} and Market Price MP_t^{sc} , we concatenate feature-wise MN_t^{sc} , MP_t^{sc} and the **Stock embedding** E^{sc} . The stock embedding E^{sc} represents the stock code of the sample on a given day t . Finally, we have a Fully Connected (FC) layer that learns the **Joint Representation** of all modes. This fixed-sized joint representation is fed into a FC layer with linear activation that predicts the next day volatility $\hat{\sigma}_{t+1}$.

Below, we detail, for each mode separately, the layers of our hierarchical model.

– Text mode

1. Word Embedding Retrieval

Standard embedding layer with no trainable parameters. It receives a vector of word indices as input and returns a matrix of word embeddings.

2. News Encoder

This layer encodes all news on a given day and outputs a set news embeddings $\{S_t^1, \dots, S_t^{l_n}\}$. Each encoded sentence has dimension d_S , which is a hyperparameter of our model. This layer constitutes a key component of our neural architectures and, as such, we evaluate our models considering sentence encoders trained end-to-end, using the BiLSTM attention (subsubsection 4.3.2) and BiLSTM max-pooling (subsubsection 4.3.1) architectures, and also transferred from the RCV1 and SNLI as fixed features.

3. Daily news relevance attention

Our proposed **news relevance** attention mechanism for all news released on a given day. The attention mechanism is introduced to tackle information

¹³The headline encoding S_t is learnt end-to-end from the headline word embeddings or transferred from the TL tasks as fixed features.

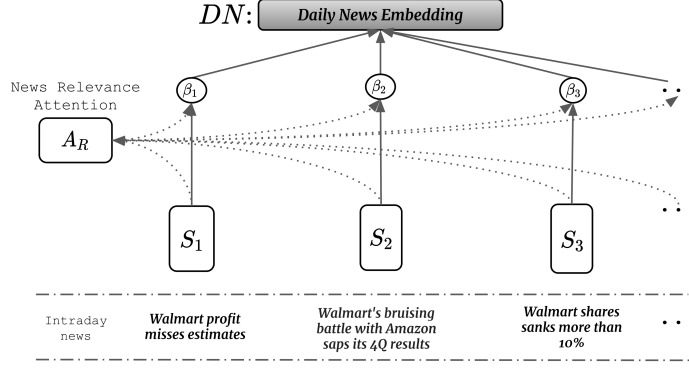


Figure 6: **Daily news relevance attention.** The figure illustrates a day where three news were released for the Walmart company. After the headlines are encoded into a fixed-size representation S , the daily *news relevance attention* A_R converts all sentences into single vector representation of all Daily News DN by attending each headline based on its content.

overload. It was designed to “filter out” redundant or misleading news and focus on the relevant ones based solely on the news content. Formally, the layer outputs a Daily News (DN) embedding $DN_t^{sc} = \sum_{i=1}^{l_n} \beta_i S_t^{sc^i}$, which is a linear combination of all encoded news on a given day t . This news-level attention uses the same equations as in Equation 31, but with trainable weights $\{W_R, b_R, v_R\}$, i.e. the weights are segregated from the sentence encoder. Figure 6, illustrates our relevance attention. Note that this layer was deliberately developed to be invariant to headlines permutation, as is the case with the linear combination formula above. The reason is that our price data is sampled daily and, as a consequence, we are not able to discriminate the market reaction for each intraday news.

4. News Temporal Context

Sequence layer with daily news embeddings DN_t^{sc} as time steps. This layer aims to learn the temporal context of news, i.e. the relationship between the news at day t and the T past days. It receives as input a chronologically ordered sequence of T past Daily News embeddings $\{DN_{t-T}^{sc}, \dots, DN_t^{sc}\}$ and outputs the news mode encoding Market News $MN_t^{sc} \in d_{MN}$. The sequence with T time steps is encoded using a BiLSTM attention. The layer was designed to capture the temporal order that news are released and the current **news novelty**. i.e. news that were repeated in the past can be “forgotten” based on the modulating gates of the LSTM network.

– **Price mode**

5. Price Encoder

Sequence layer analogous to **News Temporal Context**, but for the price mode. The input is the ordered sequence Daily Prices $\{DP_{t-T}^{sc}, \dots, DP_t^{sc}\}$ of

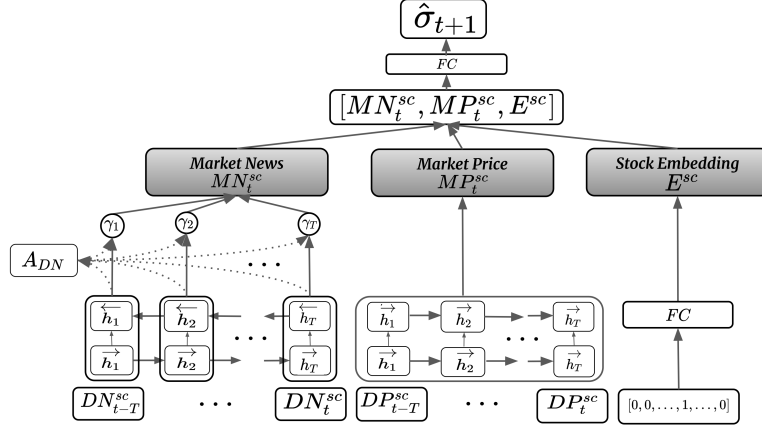


Figure 7: **Hierarchical Neural Network architecture.**

size T , where each element the price feature defined in Equation 33. Particularly, the architecture consists of two stacked LSTM's. The first one outputs for each price feature time step a hidden vector that takes the temporal context into account. Then these hidden vectors are again passed to a second independent LSTM. The layer outputs the price mode encoding Market Price $MP_t^{sc} \in d_{MP}$. This encoding is the last hidden vector of the second LSTM Market.

– **Stock embedding**

6. **Stock Encoder**

Stock dense representation. The layer receives the discrete encoding \mathcal{I}_t^{sc} indicating the sample stock code pass through a FC layer and outputs a stock embedding E_{sc} .

– **Joint Representation**

7. **Merging**

Feature-wise News, Price, and Stock modes concatenation. No trainable parameters.

7. **Joint Representation Encoder**

FC layer of size d_{JR} .

5.4. *Multimodal learning with missing modes*

During the training we feed into our neural model the price, news, and stock indicator data. The price and stock indicator modes data occur in all days. However, at the individual stock level we can have days that the company is not covered by the media. This feature imposes challenges to our multimodal training since neural networks are not able to handle missing modes without special intervention. A straightforward solution would be to consider only days with news released, disregarding the remaining samples. However, this approach

has two main drawbacks. First, the “missing news” do not happen at random, or are attributed to measurement failure as is, for example, the case of multimodal tasks using mechanical sensors data. Conversely, as highlighted in [8, 9] the same price behaviour results in distinct market reactions when accompanied or not by news¹⁴. In other words, specifically to financial forecasting problems the absence or existence of news are highly informative.

Some methods were proposed in the multimodal literature to effectively treat informative missing modes or “informative missingness”, which is a characteristic refereed in the literature as *learning with missing modalities* [23]. In this work, we directly model the news missingness as a feature of our text model temporal sequence by using the method initially proposed in [46, 47] for clinical data with missing measurements and applied in the context of financial forecasting in [48]. Specifically, we implement the *Zeros & Imputation* (ZI) method [47] in order to jointly learn the price mode and news relationship across all days of market activity.

The ZI implementation is described as follows: Before the daily news sequence is processed by the text temporal layer (described in item 4) we input a 0 vector for all time steps with missing news and leave the news encoding unchanged otherwise. This step is called zero imputation. In addition, we concatenate feature-wise an indicator vector with value 1 for all vectors with zero imputation and 0 for the days with news.

As described in [48], the ZI method endow a temporal sequence model with the ability to learn different representations depending on the news history and its relative time position. Moreover, it allows our model to predict the volatility for all days of our time series and, at the same time, take into account the current and past news informative missingness. Furthermore, the learnt positional news encoding works differently than a typical “masking”, where days without news are not passed through the LSTM cell. Masking the time steps would be losing information about the presence or absence of news concomitant with prices.

6. Experimental results and discussions

We aim to evaluate our hierarchical neural model in the light of three main aspects. First, we asses the importance of the different sentence encoders to our end-to-end models and how it compares to transferring the sentence encoder from our two auxiliary TL tasks. Second, we ablate our proposed news relevance attention (NRA) component to evaluate its importance. Finally, we consider a model that takes into consideration only the price mode (unimodal), i.e. ignoring any architecture related to the text mode.

Before we define the baselines to asses the three aspects described above, we review in the next section the scores of the trained TL tasks.

¹⁴Experimental results [8, 9] demonstrate that large price dislocations in the absence of news tend revert and continue the movement (momentum) when driven by news.

6.1. Auxiliary transfer learning tasks

This section reports the performance of the auxiliary TL tasks considered in this work. Our ultimate goal is to indicate that our scores are in line with previous works

All the architectures presented in subsection 4.2 are trained for a maximum of 50 epochs using mini-batch SGD with Adam optimizer [49]. Moreover, at the end of each epoch, we evaluate the validation scores, which are accuracy (Stanfor SNLI dataset) and F1 (RCV1 dataset), and save the weights with the best values. Aiming to speed up training, we implement *early stopping* with patience set to 8 epochs. That is, if the validation scores do not improve for more than 10 epochs we halt the training. Finally, we use Glove pre-trained word embeddings [38] as fixed features.

Table 5 compares our test scores with state-of-the-art (SOTA) results reported in previous works. We can see that our scores for the SNLI task are very close to state-of-the-art¹⁵.

Regarding the RCV1 dataset, our results consider only the headline content for training, while the refereed works consider both the news headline and message body. The reason for training using only the headlines is that both tasks are learnt with the sole purpose of transferring the sentence encoders to our main volatility prediction task, whose textual input is restricted to headlines.

6.2. Training setup

During the training of our hierarchical neural model described in subsection 5.3 we took special care to guard against overfitting. To this aim, we completely separate 2016 and 2017 as the test set and report our results on this “unseen” set. The remaining data is further split into training (2007 to 2013) and validation (2014 to 2015). The model convergence during training is monitored in the validation set. We monitor the validation score of our model at the end of each epoch and store the network weights if the validation scores improves between two consecutive epochs. Additionally, we use mini-batch SGD with Adam optimizer and early stopping with patience set to eight epochs. The hyperparameter tuning is performed using grid search.

All training is performed using the proposed global model approach described in subsection 5.2, which learns a model that takes into account the features of all the 40 stocks of our corpus. Using this approach our training set has a total of 97,903 samples. Moreover, during the SGD mini-batch sampling the past T days of price and news history tensors and each stock sample stock indicator are randomly selected from the set of all 40 stocks.

6.3. Stocks universe result

In order to evaluate the contributions of each component of our neural model described in subsection 5.3 and the effect of using textual data to predict the

¹⁵Models were trained using a concatenation layer and Bidirectional LSTM with 512 and 1024 units, respectively

volatility, we report our results using the following baselines¹⁶:

1. - **News (unimodal price only)**: This baseline completely ablates (i.e. removes) any architecture related to the news mode, considering only the price encoding and the stock embedding components. Using this ablation we aim to evaluate the influence of news to the volatility prediction problem.
2. + **News (End-to-end Sentence Encoders) - NRA**: This baseline ablates our proposed new relevance attention (NRA) component, and instead, makes use of the same *Daily Averaging* method in [27, 28], where all fixed-sized headline representations on a given day are averaged without taking into account the relevance of each news. We evaluate this baseline for both BiLSTM attention (Att) and BiLSTM max-pooling (MP) sentence encoders. Here, our goal is to assess the true contribution of our NRA component in the case SOTA sentence encoders are taken into account.
3. + **News (End-to-End W-L Att Sentence Encoder) + NRA**: The Word-Level Attention (W-L Att) sentence encoder implements an attention mechanism directly on top of word embeddings, and, as such, does not consider the order of words in a sentence. This baseline complements the previous one, i.e. it evaluates the influence of the sentence encoder when our full specification is considered.
4. + **News (TL Sentence Encoders) + NRA**: Makes use of sentence encoders of our two auxiliary TL tasks as fixed features. This baseline aims to address the following questions, namely: What dataset and models are more suitable to transfer to our specific volatility forecasting problem; How End-to-End models, which are trained on top of word embeddings, perform compared to sentence encoders transferred from other tasks.

Table 6 summarizes the test scores for the ablations discussed above. Our best model is the + News (BiLSTM Att) + NRA, which is trained end-to-end and uses our full architecture. The second best model, i.e. + News (BiLSTM MP) + NRA, ranks slightly lower and only differs from the best model in terms of the sentence encoder. The former sentence encoder uses an attention layer (subsubsection 4.3.2) and the latter a max-pooling layer (subsubsection 4.3.1), where both layers are placed on top of the LSTM hidden states of each word.

Importantly, our experiments show that using news and price (multimodal) to predict the volatility improves the scores by 11% (MSE) and 9% (MAE) when compared with the News (price only unimodal) model that considers only price features as explanatory variables.

When comparing the performance of End-to-End models and the TL auxiliary tasks the following can be observed: The end-to-end models trained with the two SOTA sentence encoders perform better than transferring sentence encoder from both auxiliary tasks. However, our experiments show that the same

¹⁶Minus sign means to remove (ablate) the neural network component while plus means to include the component.

does not hold for models trained end-to-end relying on the simpler WL-Att sentence encoder, which ignores the order of words in a sentence. In other words, considering the appropriate TL task, it is preferable to transfer a SOTA sentence encoder trained on a larger dataset than learning a less robust sentence encoder in an end-to-end fashion. Moreover, initially, we thought that being the RCV1 a financial domain corpus it would demonstrate a superior performance when compared to the SNLI dataset. Still, the SNLI transfers better than RCV1. We hypothesize that the text categorization task (RCV1 dataset) is not able to capture complex sentence structures at the same level required to perform natural language inference. Particularly to the volatility forecasting problem, our TL results corroborates the same findings in [18], where it was shown that SNLI dataset attains the best sentence encoding for a broad range of pure NLP tasks, including, among other, text categorization and sentiment analysis.

Significantly, experimental results in Table 6 clearly demonstrate that our proposed *news relevance attention* (NRA) outperforms the News Averaging method proposed in previous studies [27, 28]. Even when evaluating our NRA component in conjunction with the more elementary W-L Att sentence encoder it surpass the results of sophisticated sentence encoder using a News Averaging approach. In other words, our results strongly points to the advantage of discriminating noisy from impacting news and the effectiveness of learning to attend the most relevant news.

Having analyzed our best model, we now turn to its comparative performance with respect to the widely regarded GARCH(1,1) model described in subsection 4.1.

We asses our model performance relative to GARCH(1,1) using standard loss metrics (MSE and MAE) and the regression-based accuracy specified in Equation 10 and measured in terms of the coefficient of determination R^2 . In addition, we evaluate our model across two different volatility proxies: Garman-Klass ($\widehat{\sigma_{GK}}$) (Equation 13) and Parkinson ($\widehat{\sigma_{PK}}$) (Equation 12). We note that, as reviewed in subsubsection 4.1.2, these two volatility proxies are statically efficient and proper estimators of the next day volatility.

Table 7 reports the comparative performance among our best Price + News model (+ News BiLSTM (MP) + NRA), our Price only (unimodal) model and GARCH(1,1). The results clearly demonstrate the superiority of our model, being more accurate than GRACH for both volatility proxies. We note that evaluating the GARCH(1,1) model relying on standard MSE and MAE error metrics should be taken with a grain of salt. [36] provides the background theory and arguments supporting R^2 as the metric of choice to evaluate the predictive power of a volatility model. In any case, the outperformance or our model with respect to GARCH(1,1) permeates all three metrics, name R^2 , MSE and MAE .

6.4. Sector-level results

Company sectors are expected to have different risk levels, in the sense that each sector is driven by different types of news and economic cycles. Moreover, by performing a sector-level analysis we were initially interested in understanding if the outperformance of our model with respect to GARCH(1,1) was the

result of a learning bias to a given sector or if, as turned out to be the case, the superior performance of our model spreads across a diversified portfolio of sectors.

In order to evaluate the performance per sector, we first separate the constituents stocks for each sector in Table 1. Then, we calculate the same metrics discussed in the previous section for each sector individually.

Table 8 reports our experimental results segregated by sector. We observe that the GRACH model accuracy, measured using the R^2 score, has a high degree of variability among sectors. For example, the accuracy ranges from 0.15 to 0.44 for the HealthCare and Energy sector, respectively. This high degree of variability is in agreement with previous results reported in [17], but in the context of long-term (quarterly) volatility predictions. Although the GARCH(1,1) accuracy is sector-dependent, without any exception, our model using price and news as input clearly outperforms GRACH sector-wise. This fact allow us to draw the following conclusions:

- Our model outperformance is persistent across sectors, i.e. the characteristics of the results reported in Table 7 permeates all sectors, rather than being composed of a mix of outperforming and underperforming sector contributions. This fact provides a strong evidence that our model is more accurate than GARCH(1,1).
- The proposed Global model approach discussed in subsection 5.2 is able to generalize well, i.e. the patterns learnt are not biased to a given sector or stock.

One of the limitations of our work is to rely on proxies for the volatility estimation. Although these proxies are handy if only open, high, low and close daily price data is available, having high frequency price data we could estimate the daily volatility using the sum of squared intraday returns to measure the true daily latent volatility. For example, in evaluating the performance for the one-day-ahead GARCH(1,1) Yen/Dollar exchange rate [36] reports R^2 values of 0.237 and 0.392 using hourly and five minutes sampled intraday returns, respectively. However, we believe that utilizing intraday data would further improve our model performance.

Since our experimental results demonstrate the key aspect of the *news relevance attention* to model architecture we observe that intraday data would arguably ameliorate the learning process. Having intraday data would allow us to pair each individual news release with the instantaneous market price reaction. Using daily data we are losing part of this information by only measuring the aggregate effect of all news to the one-day-ahead prediction.

7. Conclusion

We study the joint effect of stock news and prices on the daily volatility forecasting problem. To the best of our knowledge, this work is one of the first studies aiming to predict short-term (daily) rather than long-term (quarterly

or yearly) volatility taking news and price as explanatory variables and using a comprehensive dataset of news headlines at the individual stock level.

Our hierarchical end-to-end model benefits from state-of-the-art approaches to encode text information and to deal with two main challenges in correlating news with market reaction: news relevance and novelty. That is, to address the problem of how to attend the most important news based purely on its content (*news relevance attention*) and to take into account the temporal information of past news (temporal context). Additionally, we propose a multi-stock mini-batch + stock embedding method suitable to model commonality among stocks.

The experimental results show that our multimodal approach outperforms the GARCH(1,1) volatility model, which is the most prevalent econometric model for daily volatility predictions. The outperformance being sector-wise and demonstrates the effectiveness of combining price and news for short-term volatility forecasting. The fact that we outperform GARCH(1,1) for all analyzed sectors confirms the robustness of our proposed architecture and evidences that our global model approach generalizes well.

We ablated (i.e. removed) different components of our neural architecture to assess its most relevant parts. To this aim, we replaced our proposed *news relevance attention* layer, which aims to attend the most important news on a given day, with a simpler architecture proposed in the literature, which averages the daily news. We found that our attention layer improves the results. Additionally, we ablated all the architecture related to the news mode and found that news enhances the forecasting accuracy.

Finally, we evaluated different sentence encoders, including those transferred from other NLP tasks, and concluded that they achieve better performance as compared to a plain Word-level attention sentence encoder trained end-to-end. However, they do not beat state-of-the-art sentence encoders trained end-to-end.

In order to contribute to the literature of Universal Sentence Encoders, we evaluated the performance of transferring sentence encoders from two different tasks to the volatility prediction problem. We showed that models trained on the Natural Language Inference (NLI) task are more suitable to forecasting problems than a financial domain dataset (Reuters RCV1). By analyzing different architectures, we showed that a BiLSTM with max-pooling for the SNLI dataset provides the best sentence encoder.

In the future, we plan to make use of intraday prices to better assess the predictive power of our proposed models. Additionally, we would further extend our analysis to other stock market sectors.

References

- [1] F. Z. Xing, E. Cambria, R. E. Welsch, Natural language based financial forecasting: a survey, *Artificial Intelligence Review* 50 (1) (2018) 49–73. doi:10.1007/s10462-017-9588-9. URL <http://link.springer.com/10.1007/s10462-017-9588-9>

- [2] P. Milgrom, N. Stokey, Information, trade and common knowledge, *Journal of Economic Theory*.
URL <http://www.sciencedirect.com/science/article/pii/S0022053182900461>
- [3] M. Harris, A. Raviv, Differences of Opinion Make a Horse Race, *Review of Financial Studies* 6 (3) (1993) 473–506. doi:10.1093/rfs/5.3.473.
URL <http://rfs.oxfordjournals.org/content/6/3/473.abstract>
- [4] W. Antweiler, M. Z. Frank, Is All That Talk Just Noise? The Information Content of Internet Stock Message Boards, *The Journal of Finance* 59 (3) (2004) 1259–1294.
URL <http://www.jstor.org/stable/info/3694736>
- [5] T. O. Sprenger, P. G. Sandner, A. Tumasjan, I. M. Welp, News or Noise? Using Twitter to Identify and Understand Company-specific News Flow, *Journal of Business Finance & Accounting* 41 (7-8) (2014) 791–830. doi:10.1111/jbfa.12086.
URL <http://doi.wiley.com/10.1111/jbfa.12086>
- [6] D. Vayanos, P. Woolley, An Institutional Theory of Momentum and Reversal, *Review of Financial Studies* 26 (5) (2013) 1087–1145. doi:10.1093/rfs/hht014.
URL <https://academic.oup.com/rfs/article-lookup/doi/10.1093/rfs/hht014>
- [7] H. Hong, J. C. Stein, A Unified Theory of Underreaction, Momentum Trading, and Overreaction in Asset Markets, *The Journal of Finance* 54 (6) (1999) 2143–2184. doi:10.1111/0022-1082.00184.
URL <http://doi.wiley.com/10.1111/0022-1082.00184>
- [8] W. S. Chan, Stock price reaction to news and no-news: drift and reversal after headlines, *Journal of Financial Economics* 70 (2) (2003) 223–260. doi:10.1016/S0304-405X(03)00146-6.
URL <http://www.sciencedirect.com/science/article/pii/S0304405X03001466>
- [9] J. Boudoukh, R. Feldman, S. Kogan, M. Richardson, Which News Moves Stock Prices? A Textual Analysis, NBER Working Paper.
URL <http://www.nber.org/papers/w18725>
- [10] C. Antoniou, J. A. Doukas, A. Subrahmanyam, Cognitive Dissonance, Sentiment, and Momentum, *Journal of Financial and Quantitative Analysis* 48 (01) (2013) 245–275. doi:10.1017/S0022109012000592.
URL http://www.journals.cambridge.org/abstract/_S0022109012000592
- [11] Consumer Confidence Survey – technical note, Tech. rep. (2011).
URL https://www.conference-board.org/pdf/_free/press/TechnicalPDF/_4134/_1298367128.pdf

- [12] P. C. Tetlock, Giving Content to Investor Sentiment: The Role of Media in the Stock Market, *The Journal of Finance* 62 (3) (2007) 1139–1168. doi:10.1111/j.1540-6261.2007.01232.x. URL <http://doi.wiley.com/10.1111/j.1540-6261.2007.01232.x>
- [13] S. Kogan, D. Levin, B. R. Routledge, J. S. Sagi, N. A. Smith, Predicting Risk from Financial Reports with Regression, in: Annual Conference of the North American Chapter of the Association for Computational Linguistics, 2009, pp. 272–280. URL <http://www.aclweb.org/anthology/N09-1031>
- [14] C.-J. Wang, M.-F. Tsai, T. Liu, C.-T. Chang, Financial Sentiment Analysis for Risk Prediction, in: International Joint Conference on Natural Language Processing, 2013, pp. 802–808. URL <http://www.aclweb.org/anthology/I13-1097>
- [15] M.-F. Tsai, C.-J. Wang, Financial Keyword Expansion via Continuous Word Vector Representations, in: Proceedings of the 2014 Conference on Empirical Methods in Natural Language Processing (EMNLP), Association for Computational Linguistics, Stroudsburg, PA, USA, 2014, pp. 1453–1458. doi:10.3115/v1/D14-1152. URL <http://aclweb.org/anthology/D14-1152>
- [16] C. Nopp, T. Wien, A. Hanbury, Detecting Risks in the Banking System by Sentiment Analysis, in: Proceedings of the 2015 Conference on Empirical Methods in Natural Language Processing., 2015, pp. 591–600. URL <http://www.emnlp2015.org/proceedings/EMNLP/pdf/EMNLP071.pdf>
- [17] N. Rekabsaz, M. Lupu, A. Baklanov, A. Hanbury, A. Ur, L. Anderson, T. Wien, Volatility Prediction using Financial Disclosures Sentiments with Word Embedding-based IR Models, in: 55th Annual Meeting of the Association for Computational Linguistics, 2017, pp. 1712–1721. doi:10.18653/v1/P17-1157. URL <https://doi.org/10.18653/v1/P17-1157>
- [18] A. Conneau, D. Kiela, H. Schwenk, L. Barrault, A. Bordes, Supervised Learning of Universal Sentence Representations from Natural Language Inference DataarXiv:1705.02364, doi:10.1.1.156.2685. URL <http://arxiv.org/abs/1705.02364>
- [19] L. Mou, Z. Meng, R. Yan, G. Li, Y. Xu, L. Zhang, Z. Jin, How Transferable are Neural Networks in NLP Applications?arXiv:1603.06111. URL <http://arxiv.org/abs/1603.06111>
- [20] J. Howard, S. Ruder, Universal Language Model Fine-tuning for Text ClassificationarXiv:1801.06146. URL <http://arxiv.org/abs/1801.06146>

- [21] T. Loughran, B. McDonald, When is a Liability not a Liability? Textual Analysis, Dictionaries, and 10-Ks, *The Journal of Finance* 66 (1) (2011) 35–65.
URL <http://bit.ly/15GhT7K>
- [22] T. Mikolov, I. Sutskever, K. Chen, G. S. Corrado, J. Dean, Distributed Representations of Words and Phrases and their Compositionality, in: C. J. C. Burges, L. Bottou, M. Welling, Z. Ghahramani, K. Q. Weinberger (Eds.), *Advances in Neural Information Processing Systems* 26, Curran Associates, Inc., 2013, pp. 3111–3119.
URL <https://dl.acm.org/citation.cfm?id=2999959>
- [23] T. Baltrušaitis, C. Ahuja, L.-P. Morency, Multimodal Machine Learning: A Survey and Taxonomy [arXiv:1705.09406](https://arxiv.org/abs/1705.09406).
URL <http://arxiv.org/abs/1705.09406>
- [24] J. Bollen, H. Mao, X.-J. Zeng, Twitter Mood Predicts the Stock Market, *Journal of Computational Science* 2 (1) (2011) 1–8.
[arXiv:arXiv:1010.3003v1](https://arxiv.org/abs/1010.3003v1).
URL <http://www.sciencedirect.com/science/article/pii/S187775031100007X>
- [25] R. P. Schumaker, H. Chen, Textual Analysis of Stock Market Prediction Using Breaking Financial News: The AZFin Text System, *ACM Trans. Inf. Syst.* 27 (2) (2009) 12:1—12:19. doi:10.1145/1462198.1462204.
URL <http://doi.acm.org/10.1145/1462198.1462204>
- [26] T. H. Nguyen, K. Shirai, Topic Modeling based Sentiment Analysis on Social Media for Stock Market Prediction, in: *Proceedings of the 53rd Annual Meeting of the Association for Computational Linguistics*, 2015, pp. 1354–1364.
URL <http://www.aclweb.org/anthology/P15-1131>
- [27] X. Ding, Y. Zhang, T. Liu, J. Duan, Deep learning for event-driven stock prediction, in: *Proceedings of the 24th International Joint Conference on Artificial Intelligence (ICJAI 15)*, 2015, pp. 2327–2333.
URL <https://www.ijcai.org/Proceedings/15/Papers/329.pdf>
- [28] L. d. S. Pinheiro, M. Dras, Stock Market Prediction with Deep Learning: A Character-based Neural Language Model for Event-based Trading, in: *Proceedings of the Australasian Language Technology Association Workshop 2017*, 2017, pp. 6–15.
URL <https://aclanthology.coli.uni-saarland.de/papers/U17-1001/u17-1001>
- [29] J. Deng, W. Dong, R. Socher, L.-J. Li, Kai Li, Li Fei-Fei, ImageNet: A large-scale hierarchical image database, in: *2009 IEEE Conference on Computer Vision and Pattern Recognition*, IEEE, 2009, pp. 248–255.

doi:10.1109/CVPR.2009.5206848.

URL <http://ieeexplore.ieee.org/document/5206848/>

- [30] A. S. Razavian, H. Azizpour, J. Sullivan, S. Carlsson, CNN Features Off-the-Shelf: An Astounding Baseline for Recognition, in: 2014 IEEE Conference on Computer Vision and Pattern Recognition Workshops, IEEE, 2014, pp. 512–519. doi:10.1109/CVPRW.2014.131.
URL <http://ieeexplore.ieee.org/lpdocs/epic03/wrapper.htm?arnumber=6910029>
- [31] S. R. Bowman, G. Angeli, C. Potts, C. D. Manning, A large annotated corpus for learning natural language inference, in: Proceedings of the 2015 Conference on Empirical Methods in Natural Language Processing, Association for Computational Linguistics, Stroudsburg, PA, USA, 2015, pp. 632–642. doi:10.18653/v1/D15-1075.
URL <http://aclweb.org/anthology/D15-1075>
- [32] D. D. Lewis, Y. Yang, T. G. Rose, F. Li, RCV1: A New Benchmark Collection for Text Categorization Research, The Journal of Machine Learning Research 5 (2004) 361–397.
URL <http://dl.acm.org/citation.cfm?id=1005332.1005345>
- [33] R. F. Engle, Autoregressive Conditional Heteroscedasticity with Estimates of the Variance of United Kingdom Inflation, Econometrica 50 (4) (1982) 987. doi:10.2307/1912773.
URL <https://www.jstor.org/stable/1912773?origin=crossref>
- [34] T. Bollerslev, Generalized autoregressive conditional heteroskedasticity, Journal of Econometrics 31 (3) (1986) 307–327. doi:10.1016/0304-4076(86)90063-1.
URL <https://www.sciencedirect.com/science/article/pii/0304407686900631>
- [35] P. R. Hansen, A. Lunde, A forecast comparison of volatility models: does anything beat a GARCH(1,1)?, Journal of Applied Econometrics 20 (7) (2005) 873–889. doi:10.1002/jae.800.
URL <http://doi.wiley.com/10.1002/jae.800>
- [36] T. G. Andersen, T. Bollerslev, Answering the Skeptics: Yes, Standard Volatility Models do Provide Accurate Forecasts, International Economic Review 39 (4) (1998) 885. doi:10.2307/2527343.
URL <https://www.jstor.org/stable/2527343?origin=crossref>
- [37] P. Molnar, Properties of range-based volatility estimators, International Review of Financial Analysis 23 (2012) 20–29. doi:10.1016/J.IRFA.2011.06.012.
URL <https://www.sciencedirect.com/science/article/pii/S1057521911000731>

- [38] J. Pennington, R. Socher, C. D. Manning, GloVe: Global Vectors for Word Representation.
URL <https://nlp.stanford.edu/pubs/glove.pdf>
- [39] S. Hochreiter, J. Schmidhuber, Long Short-Term Memory, *Neural Computation* 9 (8) (1997) 1735–1780. doi:10.1162/neco.1997.9.8.1735.
URL <http://www.mitpressjournals.org/doi/10.1162/neco.1997.9.8.1735>
- [40] F. A. Gers, J. Schmidhuber, F. Cummins, Learning to Forget: Continual Prediction with LSTM, *Neural Computation* 12 (10) (2000) 2451–2471. doi:10.1162/089976600300015015.
URL <http://www.mitpressjournals.org/doi/10.1162/089976600300015015>
- [41] M. Schuster, K. Paliwal, Bidirectional recurrent neural networks, *IEEE Transactions on Signal Processing* 45 (11) (1997) 2673–2681. doi:10.1109/78.650093.
URL <http://ieeexplore.ieee.org/document/650093/>
- [42] S. Lai, L. Xu, K. Liu, J. Z. AAAI, U. 2015, Recurrent Convolutional Neural Networks for Text Classification., in: AAAI, 2015, pp. 2267–2273.
URL <http://www.aaai.org/ocs/index.php/AAAI/AAAI15/paper/download/9745/9552>
- [43] P. Li, W. Li, Z. He, X. Wang, Y. Cao, J. Zhou, W. Xu, Dataset and Neural Recurrent Sequence Labeling Model for Open-Domain Factoid Question Answering.
URL <https://arxiv.org/pdf/1607.06275.pdf>
- [44] Y. Liu, C. Sun, L. Lin, X. Wang, Learning Natural Language Inference using Bidirectional LSTM model and Inner-Attention **arXiv:arXiv:1605.09090v1**.
URL <https://arxiv.org/pdf/1605.09090.pdf>
- [45] Z. Lin, M. Feng, C. Nogueira, D. Santos, M. Yu, B. Xiang, B. Zhou, Y. Bengio, A Structured Self-Attentive Sentence Embedding, in: ICLR, 2017.
URL <https://arxiv.org/pdf/1703.03130.pdf>
- [46] Z. C. Lipton, D. C. Kale, C. Elkan, R. Wetzel, Learning to Diagnose with LSTM Recurrent Neural Networks, in: ICLR, 2016. **arXiv:1511.03677**.
URL <http://arxiv.org/abs/1511.03677>
- [47] Z. C. Lipton, D. Kale, R. Wetzel, Directly Modeling Missing Data in Sequences with RNNs: Improved Classification of Clinical Time Series, in: Proceedings of the 1st Machine Learning for Healthcare Conferenc, 2016, pp. 253–270.
URL <http://proceedings.mlr.press/v56/Lipton16.html>

- [48] J. Alberg, Z. C. Lipton, Improving Factor-Based Quantitative Investing by Forecasting Company Fundamentals, in: 31st Conference on Neural Information Processing Systems (NIPS), 2017. [arXiv:1711.04837](#).
URL <http://arxiv.org/abs/1711.04837>
- [49] D. P. Kingma, J. Lei Ba, Adam: A method for stochastic optimization, in: ICLR, 2015. [arXiv:arXiv:1412.6980v9](#).
URL <https://arxiv.org/pdf/1412.6980.pdf>
- [50] R. Johnson, T. Zhang, Effective Use of Word Order for Text Categorization with Convolutional Neural Networks, in: NAACL, 2015, pp. 103–112.
URL <http://www.anthology.aclweb.org/N/N15/N15-1011.pdf>

Sector ETF	Constituent Stocks
Consumer Staples (XLP)	Procter & Gamble (PG), Coca-Cola Company (KO), PepsiCo (PEP), Walmart (WMT), Costco Wholesale Corporation (COST), CVS Health Corporation (CVS), Altria Group (MO), Walgreens Boots Alliance (WBA), Mondelez International (MDLZ), Colgate-Palmolive (CL),
Energy (XLE)	Exxon-Mobil (XOM), Chevron (CVX), ConocoPhillips (COP), EOG Resources (EOG), Occidental Petroleum Corporation (OXY), Valero Energy Corporation (VLO), Halliburton Company (HAL), Schlumberger Limited (SLB), Pioneer Natural Resources (PXD), Anadarko Petroleum Corporation (APC)
Utilities (XLU)	NextEra Energy (NEE), Duke Energy (DUK), The Southern Company (SO), Dominion Energy (D), Exelon Corporation (EXC), American Electric Power Company (AEP), Sempra Energy (SRE), Public Service Enterprise Group (PEG), Consolidated Edison (ED), Xcel Energy (XEL)
Healthcare (XLV)	Johnson & Johnson (JNJ), UnitedHealth Group (UNH), Pfizer (PFE), Merck & Co. (MRK), Medtronic (MDT), Amgen (AMGN), Abbott Laboratories (ABT), Gilead Sciences (GILD), Eli Lilly (LLY), Bristol-Myers Squibb (BMY)
Financials (XLF)	Berkshire Hathaway (BRK-A), JPMorgan Chase (JPM), Bank of America Corporation (BAC), Wells Fargo (WFC), CitiBank (C), Goldman Sachs Group (GS), U.S. Bancorp (USB), Morgan Stanley (MS), American Express (AXP), PNC Financial Services Group (PNC)

Table 1: **Corpus sectors and respective constituent stocks.** For each sector we selected the top 10 stock holdings (as in January 2018). Stock codes in parentheses.

Sector ETF	before market	during market	after market
Consumer Staples	54%	31%	15%
Energy	44%	36%	20%
Utilities	58%	31%	11%
Healthcare	55%	28%	17%
Financials	63%	24%	13%
<i>total</i>	84,556	40,996	21231

Table 2: **Distribution of headlines per sector according to market hours.** The majority of the 146,783 headlines are released before 9:30AM (**before market**). The category **after market** includes news released after 4:00PM EDT. We count the categories **holiday** and **weekend** as **before market** since they impact the following working day.

Date and time	Headline
2011-12-13 00:18:39 EDT	<i>Valero reports power outage at Port Arthur refinery</i>
2007-04-17 08:54:27 EDT	<i>Wells Fargo profit rises 11 pct on commercial loans</i>
2017-12-14 14:40:31 EDT	<i>Perrigo lines up bid for Merck’s consumer health unit</i>
2007-01-03 10:27:42 EDT	<i>UPDATE 1-Bear Stearns ups Merck to outperform</i>
2010-02-23 13:35:11 EDT	<i>Exxon Mobil says remains bullish on Nigeria</i>
2016-09-22 15:32:13 EDT	<i>Texas regulators express “deep concern” over NextEra deal</i>
2008-10-14 08:30:00 EDT	<i>Smart For LifeTM Now Available on Costco.com</i>

Table 3: **Random samples from our dataset.** Note the factual/objective characteristic of our corpus, where typical news do not carry any sentiment connotation.

Premise	Hypothesis	Label
Children smiling and waving at camera.	There are children present.	e
Two blond women are hugging one another.	Some women are hugging on vacation.	n
A farmer fertilizing his garden with manure with a horse and wagon.	The man is fertilizing his garden.	e
The furry brown dog is swimming in the ocean.	A dog is running around the yard.	c
A dog drops a red disc on a beach.	a dog catch the ball on a beach.	c
Several armed forces officers and civilians are standing around a children’s playground.	Civilians and armed forces officers trade insults at a playground.	n

Table 4: **Stanford NLI (SNLI) dataset examples.** Natural language sentence pairs are labelled with entailment (e), contradiction (c), or neutral (n).

Dataset	Sentence Encoder	Score
<i>SNLI</i>	LSTM original paper ([31])	0.806
	BiLSTM over Mean Pooling ([44])	0.833
	BiLSTM attention (Att) with multiple views and factored fusion layer ([45])	0.844
	BiLSTM max-pooling (MP) with sentence embedding size 4096 ([18])	0.845
	Our BiLSTM Att with sentence embedding size 2048	<u>0.838</u>
	Our BiLSTM MP with sentence embedding size 2048	<u>0.841</u>
<i>RCV1</i>	k -NN [†] ([32])	0.765
	Best Support Vector Machine (SVM) [†] ([32])	0.816
	bow-CNN [†] ([50])	0.840
	Our BiLSTM Att with sentence embedding size 2048 (headlines only)	<u>0.809</u>
	Our BiLSTM MP with sentence embedding size 2048 (headlines only)	<u>0.811</u>

Table 5: **TL auxiliary tasks – Sentence Encoders comparison.** Test scores are accuracy and F1 scores for the SNLI subsection 4.2.2 and RCV1 subsection 4.2.1 datasets, respectively. † indicates model trained with both headlines and body content and using the original 103 classes of the RCV1 dataset, rather than our models that are trained using headlines only and a total of 55 classes (see subsection 4.2.1 for a complete description). As a consequence, the reported benchmarks for the RCV1 dataset are not directly comparable and where reported for the sake of a better benchmark.

Model	MSE	MAE
All stocks		
- News (price only unimodal) [†]	2.140E-05	3.093E-03
+ News (BiLSTM Att) - <i>news relevance attention</i> (NRA)	2.078E-03	3.037E-03
+ News (BiLSTM MP) - NRA	2.077E-03	3.031E-03
+ News (TL Reuters RCV1 BiLSTM MP) + NRA	2.037E-03	3.020E-03
+ News (TL Reuters RCV1 BiLSTM Att) + NRA	2.023E-03	3.011E-03
+ News (W-L Att) ^{††} + NRA	2.006E-03	2.947E-03
+ News (TL SNLI BiLSTM Att) + NRA	1.986E-03	2.926E-03
+ News (TL SNLI BiLSTM MP) + NRA	1.974E-03	2.918E-03
+ News (BiLSTM MP) + NRA	1.904E-03	2.851E-03
+ News (BiLSTM Att) + NRA	1.898E-03	2.823E-03

Table 6: **Model architecture ablations and sentence encoders comparisons.** The minus sign means that the component of our network architecture described in subsection 5.3 was ablated (i.e. removed) and the plus sign that it is added. The second and third row report results replacing the *news relevance attention* (NRA) with a News Averaging component as in [27, 28]. [†] indicates our model was trained using only the price mode. ^{††} highlights that the sentence encoder Word-Level Attention (W-L Attention) does not take into consideration the headline words order. Best result in bold.

Model	Vol Estimator	R^2	MSE	MAE
All Stocks				
<i>GARCH(1,1)</i>	$\widehat{\sigma_{GK}}$	0.357	2.46E-05	3.16E-03
	$\widehat{\sigma_{PK}}$	0.329	2.57E-05	3.20E-03
<i>Our Model: Price (Unimodal)</i>	$\widehat{\sigma_{GK}}$	0.384	2.14E-05	3.09E-03
	$\widehat{\sigma_{PK}}$	0.350	2.36E-05	3.29E-03
<i>Our Model: Price + News</i>	$\widehat{\sigma_{GK}}$	0.455	1.90E-05	2.82E-03
	$\widehat{\sigma_{PK}}$	0.410	2.09E-05	2.98E-03

Table 7: **Our volatility model performance compared with GARCH(1,1).** Best performance in bold. Our model has superior performance across the three evaluation metrics and taking into consideration the state-of-the-art volatility proxies, namely Garman-Klass ($\widehat{\sigma_{PK}}$) and Parkinson ($\widehat{\sigma_{PK}}$).

Model	Vol Estimator	R^2	MSE	MAE
Consumer Staples				
<i>GARCH(1,1)</i>	$\widehat{\sigma_{GK}}$	0.173	2.01E-05	2.63E-03
	$\widehat{\sigma_{PK}}$	0.155	2.08E-05	2.70E-03
<i>Our Model: Price (Unimodal)</i>	$\widehat{\sigma_{GK}}$	0.194	1.93E-05	2.67E-03
	$\widehat{\sigma_{PK}}$	0.176	2.04E-05	2.82E-03
<i>Our Model: Price + News</i>	$\widehat{\sigma_{GK}}$	0.224	1.80E-05	2.48E-03
	$\widehat{\sigma_{PK}}$	0.201	1.90E-05	2.61E-03
HealthCare				
<i>GARCH(1,1)</i>	$\widehat{\sigma_{GK}}$	0.150	2.20E-05	3.05E-03
	$\widehat{\sigma_{PK}}$	0.138	2.33E-05	3.09E-03
<i>Our Model: Price (Unimodal)</i>	$\widehat{\sigma_{GK}}$	0.186	2.01E-05	3.01E-03
	$\widehat{\sigma_{PK}}$	0.164	2.24E-05	3.21E-03
<i>Our Model: Price + News</i>	$\widehat{\sigma_{GK}}$	0.258	1.76E-05	2.74E-03
	$\widehat{\sigma_{PK}}$	0.225	1.96E-05	2.90E-03
Financials				
<i>GARCH(1,1)</i>	$\widehat{\sigma_{GK}}$	0.274	2.02E-05	3.14E-03
	$\widehat{\sigma_{PK}}$	0.250	2.17E-05	3.18E-03
<i>Our Model: Price (Unimodal)</i>	$\widehat{\sigma_{GK}}$	0.326	1.77E-05	3.10E-03
	$\widehat{\sigma_{PK}}$	0.290	2.03E-05	3.32E-03
<i>Our Model: Price + News</i>	$\widehat{\sigma_{GK}}$	0.373	1.65E-05	2.84E-03
	$\widehat{\sigma_{PK}}$	0.332	1.86E-05	3.00E-03
Energy				
<i>GARCH(1,1)</i>	$\widehat{\sigma_{GK}}$	0.443	4.38E-05	4.24E-03
	$\widehat{\sigma_{PK}}$	0.412	4.52E-05	4.27E-03
<i>Our Model: Price (Unimodal)</i>	$\widehat{\sigma_{GK}}$	0.440	3.60E-05	4.13E-03
	$\widehat{\sigma_{PK}}$	0.406	3.98E-05	4.34E-03
<i>Our Model: Price + News</i>	$\widehat{\sigma_{GK}}$	0.538	3.04E-05	3.72E-03
	$\widehat{\sigma_{PK}}$	0.495	3.38E-05	3.88E-03
Utilities				
<i>GARCH(1,1)</i>	$\widehat{\sigma_{GK}}$	0.167	1.71E-05	2.75E-03
	$\widehat{\sigma_{PK}}$	0.154	1.75E-05	2.77E-03
<i>Our Model: Price (Unimodal)</i>	$\widehat{\sigma_{GK}}$	0.145	1.40E-05	2.56E-03
	$\widehat{\sigma_{PK}}$	0.128	1.51E-05	2.75E-03
<i>Our Model: Price + News</i>	$\widehat{\sigma_{GK}}$	0.225	1.24E-05	2.34E-03
	$\widehat{\sigma_{PK}}$	0.193	1.34E-05	2.51E-03

Table 8: Sector-level performance comparison.